$Li_{13.7}Rh_8Si_{18.3}$ – A Non-Centrosymmetric Variant of the R-Phase Structure

Tim Dinges, Rolf-Dieter Hoffmann, and Rainer Pöttgen

Institut für Anorganische und Analytische Chemie, Universität Münster, Corrensstraße 30, 48149 Münster, Germany

Reprint requests to R. Pöttgen. E-mail: pottgen@uni-muenster.de

Z. Naturforsch. **2010**, *65b,* 537 – 542; received March 1, 2010

The silicide $Li_{13.7}Rh_8Si_{18.3}$ was synthesized from the elements in a sealed niobium ampoule at 1370 K followed by slow cooling. The sample was studied by powder and single-crystal X-ray diffraction. $Li_{13.7}Rh_8Si_{18.3}$ crystallizes with a non-centrosymmetric occupancy variant of the R-phase structure $Mg_{32}(Al, Zn)_{49}$: $I23$, $a = 1306.9(2)$ pm, $wR2 = 0.0447$, 1286 F^2 values, and 53 variables. Striking structural motifs of the $Li_{13.7}Rh_8Si_{18.3}$ structure are M_{12} icosahedra and M_{60} buckyball-type clusters (M = Si + Rh), both partially built up from mixed-occupied sites.

Key words: Lithium, Silicide, Group-Subgroup, Crystal Structure

Introduction

Lithium transition metal (T) stannides have intensively been studied in recent years with respect to their crystal chemistry and lithium mobility, aiming for electrode materials for lithium batteries [1 – 24]. The use of intermetallic lithium compounds instead of elemental lithium has two main reasons, (i) the dendrite growth upon lithium reduction is reduced and (ii) the charge transfer from lithium to a polyanionic network strongly increases the melting point of the materials which is a significant safety aspect. To give an example, from elemental lithium to $Li_{22}Sn_5$, the melting point increases from 181 to 783 °C [25]. Similar trends occur for ternary compounds.

The structural chemistry of the $Li_xT_ySn_z$ stannides has a common principle. The transition metal and tin atoms build up two- or three-dimensional polyanionic, covalently bonded $[T_ySn_z]^{\delta-}$ networks which are separated and charge-balanced by the lithium ions. The charge transfer from lithium to the transition metal and tin atoms enables the formation of the polyanions. Most compounds show a precise composition, while extended solid solutions have been observed for the series $Li_{3-x}Pt_2Sn_{3+x}$ [14], $Li_{1.42(5)}Pd_2Sn_{5.58(5)}$ [19], and $Li_xT_3Sn_{7-x}$ (T = Rh, Ir) [21]. Mixed-occupied sites and/or vacancies are a good prerequisite for lithium mobility. Such sites have more frequently been observed for the family of lithium transition metal silicides. So far the silicides $Li_5Ni_4Si_7$ [26], $Li_{13}Ni_{40}Si_{31}$ [27], $Li_{77-x}Ni_{20}Si_{135-y}$ (x = 2; y = 7) [28], LiCuSi [26, 29], $LiCu_2Si$ [1, 3], $LiCu_3Si_2$ [30], $Li_{119}Cu_{145}Si_{177}$ [31], $Li_{113}Cu_{54}Si_{57}$ [32], $Li_7Cu_7Si_5$ [33], Li_2ZnSi [34, 35], $LiRh_2Si$ [36], $Li_{13}Pd_{12}Si_{12}$ [37], $LiPdSi_3$ [38], $Li_8Ag_3Si_5$ [29], $Li_8Au_3Si_5$ [29], Li_2AuSi [2], and $LiRh_2Si_2$ [39] have been reported. Especially the nickel- and copper-containing phases exhibit large unit cells with substantial disorder. In continuation of our phase analytical investigations of the Li-Rh-Si system, besides $LiRh_2Si_2$ [39] and $Li_3Rh_4Si_4$ [40], we have obtained a new complex silicide $Li_{13.7}Rh_8Si_{18.3}$, which is structurally related with the R-phase structures [26, 41 – 50], originally determined for $Mg_{32}(Al, Zn)_{49}$ [41, 42], and later on for the lithium-containing phases $Li_{2.9}CuAl_{5.6}$ [43], R-Li_3CuAl_5 [44], $Li_{13}Cu_6Ga_{21}$ [45], and the extended solid solution $(Li, Mg)_{1.63}(Zn, Al)_{3.37}$ [49]. Herein we report on the synthesis and structure of $Li_{13.7}Rh_8Si_{18.3}$.

Experimental Section

Synthesis

Starting materials for the preparation of the $Li_{13.7}Rh_8Si_{18.3}$ sample were lithium rods (Merck, > 99 %), rhodium powder (Heraeus, *ca.* 200 mesh, > 99.9 %) and silicon lumps (Wacker, > 99.9 %). The lithium rods were cut into smaller pieces under dry paraffin oil and subsequently washed with *n*-hexane. The lithium pieces were kept in Schlenk tubes under argon prior to the reaction. Argon was purified with titanium sponge (900 K), silica gel, and

Table 1. Crystal data and structure refinement for $Li_{13.7}Rh_8Si_{18.3}$.

Empirical formula	$Li_{13.7}Rh_8Si_{18.3}$
Crystal size, μm^3	$50 \times 50 \times 100$
Formula weight, g mol^{-1}	1435.0
Crystal system	cubic
Space group	$I23$
Unit cell dimensions (Guinier powder data)	
a, pm	1306.9(2)
Cell volume, V, nm^3	0.2232
Formula units per cell, Z	4
$F(000)$, e	2634
Calculated density, g cm^{-3}	4.27
Diffractometer	Stoe IPDS-II
Radiation; λ, Å	MoK_α; 0.71073
Monochromator	oriented graphite
Detector distance, mm	80
Exposure time, min	20
ω range; increment, deg	0 – 180; 1.0
Integration parameters A, B, EMS	13.5, 3.5, 0.012
θ range for data collection, deg	2 – 32
hkl range	±19, ±19, ±18
Absorption coefficient, mm^{-1}	6.8
Transmission ratio (max/min)	1.08
Total no. of reflections	13174
Independent reflections / R_{int}	1286 / 0.0309
Reflections with $I \geq 2\,\sigma(I)$ / R_{sigma}	1215 / 0.0212
Data / ref. parameters	1286 / 53
Final $R1$ / $wR2$ indices [$I \geq 2\,\sigma(I)$]	0.0206 / 0.0442
$R1$ / $wR2$ indices (all data)	0.0232 / 0.0447
Goodness-of-fit on F^2	1.002
BASF	0.21(4)
Extinction coefficient	0.00126(6)
Largest diff. peak / hole, e $\times$ 10^{-6} pm^{-3}	1.01 / −1.38

molecular sieves. The lithium pieces were mixed with the rhodium powder and the silicon lumps in the 16:9:15 atomic ratio under flowing argon, and then arc-welded [51] in a niobium ampoule under an argon pressure of about 700 mbar. The niobium tube was subsequently enclosed in an evacuated silica tube for oxidation protection. The sample was heated to 1370 K within 5 h and kept at this temperature for 1 h. Thereafter the tube was rapidly cooled to 973 K within 1 h. After three days of annealing at 973 K, the furnace was slowly cooled to r. t. at a rate of 1 K min^{-1}. The sample could readily be separated from the tube. No reaction with the container material was observed. The sample is stable in air for several days and was kept in argon-filled Schlenk tubes for best conservation. Single crystals exhibit metallic lustre and could be easily separated from the bulk material. Powders are dark grey.

EDX data

Semiquantitative EDX analyses of the crystal investigated on the diffractometer was carried out with a Leica 420i scanning electron microscope with Rh and SiO_2 as standards. The experimentally observed composition (33±3 at.-% Rh : 67±3 at.-% Si) was close to the composition obtained from the single-crystal refinement of 30.4 at.-% Rh : 69.6 at.-% Si. No impurity elements were observed. The uncertainty of the semiquantitative analyses arises from the irregular surface of the crystal. The lithium content could not be determined *via* EDX (detectability limit of the instrument).

Table 2. Atomic coordinates and isotropic displacement parameters (pm^2) for $Li_{13.7}Rh_8Si_{18.3}$. U_{eq} is defined as one third of the trace of the orthogonalized U_{ij} tensor. $M1$ and $M2$ have occupancies of (0.78(1)Si / 0.22(1)Li) and (0.338(3)Rh / 0.662(3)Si), respectively.

Atom	W.-position	x	y	z	U_{eq} / U_{iso}
Li1	8*c*	0.1908(5)	x	x	109(19)
Li2	24*f*	0.9973(6)	0.3050(5)	0.1226(5)	143(11)
Li3	12*e*	0.1974(7)	0	1/2	137(16)
Li4	8*c*	0.8092(5)	x	x	121(20)
Rh	24*f*	0.84704(2)	0.81234(2)	0.58869(2)	90(1)
Si1	24*f*	0.16047(7)	0.19192(8)	0.40139(7)	74(2)
Si2	24*f*	0.99961(8)	0.17667(7)	0.31054(7)	80(2)
$M1$	12*e*	0.4007(1)	0	1/2	111(5)
$M2$	24*f*	0.99983(5)	0.09099(4)	0.15186(4)	109(2)

X-Ray diffraction

The polycrystalline $Li_{13.7}Rh_8Si_{18.3}$ sample was characterized through a Guinier pattern (imaging plate detector, Fujifilm BAS-1800) with Cu$K_{\alpha1}$ radiation and α-quartz (a = 491.30, c = 540.46 pm) as an internal standard. The lattice parameter was deduced from a least-squares fit to the powder data. Correct indexing of the pattern was ensured by an intensity calculation [52]. The powder (a = 1306.9(2) pm) and single-crystal (a = 1305.9(2) pm) lattice parameters agreed well.

Well-shaped single crystals of $Li_{13.7}Rh_8Si_{18.3}$ were isolated from the bulk material under a light microscope, glued to quartz fibres using bees wax and then investigated *via* Laue photographs on a Buerger camera (white Mo radiation) in order to check their quality. Intensity data of a suitable crystal were collected with graphite-monochromatized MoK_α radiation on a Stoe IPDS-II diffractometer in oscillation mode. A numerical absorption correction was applied to the data set. All relevant crystallographic data for the data collection and evaluation are listed in Table 1.

Structure determination and refinement

Careful examination of the $Li_{13.7}Rh_8Si_{18.3}$ data set showed a body-centered cubic cell with low Laue symmetry and no further systematic extinctions, leading to space groups $I\bar{3}m$ and $I23$, of which the non-centrosymmetric group was found to be correct during structure refinement. The starting atomic positions of the rhodium and silicon sites were obtained through Direct Methods with SHELXS-

Table 3. Interatomic distances (pm), for $Li_{13.7}Rh_8Si_{18.3}$ (calculated with the powder lattice parameters, standard deviations are all equal or smaller than 0.2 pm for the Rh–Si, Rh–Rh, and Si–Si distances and $\leq$1.5 pm for the Li–Li, Li–Si, and Li–Rh distances). All distances of the first coordination spheres are listed.

Rh:	1	Si2	239.4	*M*1:	2	Rh	258.3
	1	Si1	245.1		1	*M*1	259.5
	1	Si1	250.3		1	Li3	265.7
	1	Si2	251.3		2	Si2	267.5
	1	Si1	251.9		2	Si1	274.3
	1	*M*1	258.3		2	Li3	288.8
	1	Li3	275.6		2	Li2	326.4
	1	Li3	277.4		2	Li2	329.2
	1	Li2	280.7	Li1:	1	Li4	268.0
	1	Li2	281.6		3	Si1	278.1
	1	Li1	291.1		3	*M*2	286.1
	1	Li4	292.4		3	Rh	291.1
*M*2:	1	Si2	235.7		3	Si2	295.4
	1	*M*2	237.8		3	Li2	306.9
	2	*M*2	244.4	Li2:	1	Li3	272.9
	2	*M*2	244.9		1	Si1	276.6
	1	Li2	281.0		1	Si2	277.9
	1	Li2	282.4		1	Rh	280.7
	1	Li2	284.3		1	*M*2	281.0
	1	Li4	285.3		1	Rh	281.6
	1	Li1	286.1		1	*M*2	282.4
Si1:	1	Si2	242.3		1	*M*2	284.3
	1	Rh	245.1		1	Si2	284.4
	1	Si2	248.6		1	Si1	288.1
	1	Rh	250.3		1	Si2	297.5
	1	Rh	251.9		1	Li4	301.9
	1	*M*1	274.3		1	Li1	306.9
	1	Li4	275.3		1	Li2	320.5
	1	Li2	276.6		1	*M*1	326.4
	1	Li1	278.1		1	*M*1	329.2
	1	Li3	285.5	Li3:	1	*M*1	265.7
	1	Li3	286.1		2	Li2	273.0
	1	Li2	288.1		2	Rh	275.6
Si2:	1	*M*2	235.7		2	Rh	277.4
	1	Rh	239.4		2	Si1	285.5
	1	Si1	242.3		2	Si1	286.1
	1	Si1	248.6		2	*M*1	288.8
	1	Rh	251.3		2	Si2	297.3
	1	*M*1	267.5	Li4:	1	Li1	268.0
	1	Li2	277.9		3	Si1	275.3
	1	Li2	284.4		3	*M*2	285.8
	1	Li4	294.6		3	Rh	292.4
	1	Li1	295.4		3	Si2	294.6
	1	Li3	297.3		3	Li2	301.1
	1	Li2	297.5				

97 [53], and the structure was refined with full-matrix least-squares on F^2 using SHELXL-97 [54] with anisotropic atomic displacement parameters for these atoms. The lithium sites were subsequently located from difference Fourier syntheses and refined with isotropic displacement parameters. One of the 24*f* sites and one 12*e* site initially refined with the scattering power of rhodium and silicon showed enhanced equivalent isotropic displacement parameters, indicating lower scattering power. Consequently, we refined these sites with mixed Rh/Si and Si/Li occupancies. All other sites were fully occupied within two standard deviations and in the final cycles the ideal occupancy parameters were used. Assuming the two mixed-occupied sites we refined a composition $Li_{13.7}Rh_8Si_{18.3}$ for the investigated crystal.

Inspection of the Pearson code (cI160) revealed similarity with the R-phase structures [26, 41 – 50], however, these intermetallics adopt the centrosymmetric space group $I\bar{3}m$, a supergroup of *I*23. Subsequently we tried to refine the structure also with a centrosymmetric R-phase-related model in space group $Im\bar{3}$ with mixed-occupied sites. This refinement, however, revealed a strongly enhanced residual *R*1 of 0.1826 for all data, expressing the strong anomalous dispersion contribution of the rhodium atoms. This was a clear hint for the non-centrosymmetricity of the structure. Refinement of the correct absolute structure was ensured through a calculation of the Flack parameter [55, 56]. The latter pointed to twinning by inversion. Consequently the inversion twin matrix was introduced and a batch scale factor was refined (Table 1). A final difference Fourier synthesis revealed no significant residual peaks. The refined atomic positions, displacement parameters, and interatomic distances are given in Tables 2 and 3.

Further details of the crystal structure investigation may be obtained from Fachinformationszentrum Karlsruhe, 76344 Eggenstein-Leopoldshafen, Germany (fax: +49-7247-808-666; e-mail: crysdata@fiz-karlsruhe.de, http://www.fiz-informationsdienste.de/en/DB/icsd/depot_anforderung.html) on quoting the deposition number CSD-421555.

Discussion

The ternary silicide $Li_{13.7}Rh_8Si_{18.3}$ crystallizes with a new structure type which can be considered a non-centrosymmetric, ordered version of the R-phase structure [41, 42]. This new ordering variant and the prototype $Mg_{32}(Al, Zn)_{49}$ are related by a group-subgroup scheme (Fig. 1) [57 – 59]. Space group *I*23 is a *translationengleiche* subgroup of $Im\bar{3}$. This readily explains the twinning by inversion observed for the investigated crystal. Since $Li_5Ni_4Si_7$ [26] is crystal-chemically better related to $Li_{13.7}Rh_8Si_{18.3}$, the group-subgroup scheme presented in Fig. 1 was worked out for this pair of compounds. The 1 : 1 Rh/Si ordering on the *M*1 site of $Li_5Ni_4Si_7$ is the main reason for the lowering of the symmetry. This way the 48*h* site is split into two 24*f* sites. Furthermore we observe splitting of the 16*f* lithium site. The mixed-occupied 24*h* *M*2 site of $Li_5Ni_4Si_7$ remains a mixed-occupied site *M*2 also in $Li_{13.7}Rh_8Si_{18.3}$. In contrast to $Li_5Ni_4Si_7$ we observe a small Si/Li mixed occupancy for one 12*e*

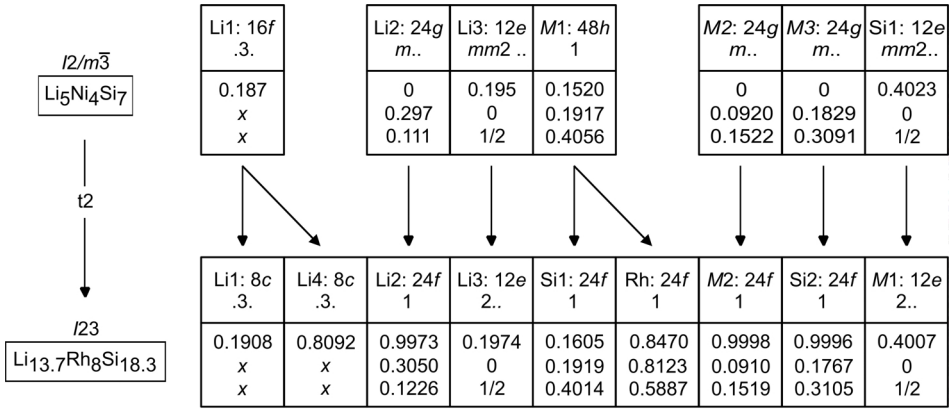

Fig. 1. Group-subgroup scheme in the Bärnighausen formalism [57 – 59] for the structures of $Li_5Ni_4Si_7$ [26] and $Li_{13.7}Rh_8Si_{18.3}$. The index for the *translationengleiche* symmetry reduction (t) and the evolution of the atomic parameters is given. For the mixed-occupied sites in the $Li_{13.7}Rh_8Si_{18.3}$ structure see Table 2.

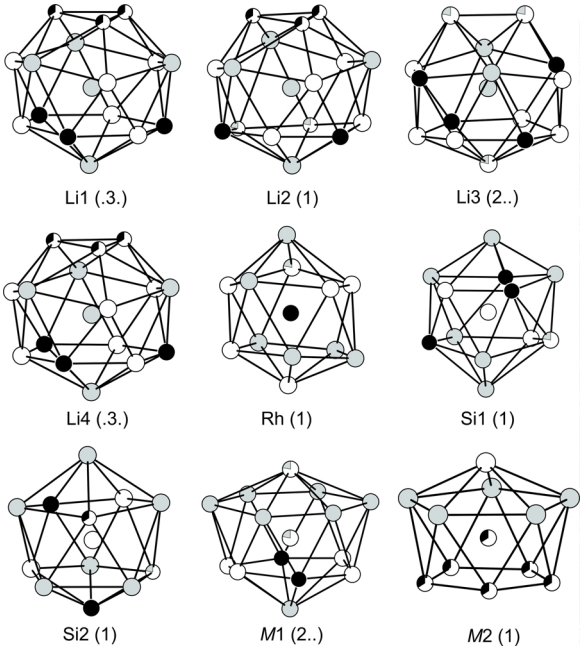

Fig. 2. Coordination polyhedra in the structure of $Li_{13.7}Rh_8Si_{18.3}$. Site symmetries are given in parentheses. For the mixed-occupied sites *M* see Table 2.

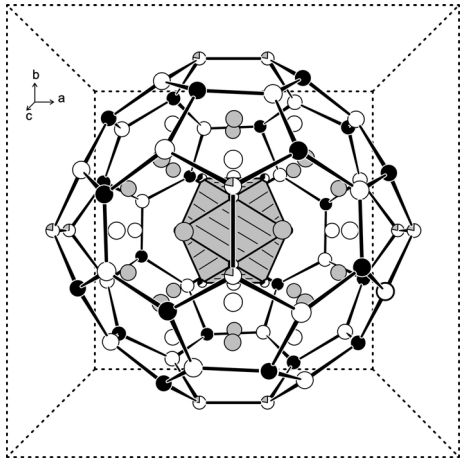

Fig. 3. Perspective view of the $Li_{13.7}Rh_8Si_{18.3}$ structure along the crystallographic *z* axis. Atom labels correspond to Fig. 2. The inner icosahedron and the Samson-type outer polyhedron are emphasized.

site which is fully occupied by silicon in the nickel compound.

The coordination polyhedra of the nine crystallographically independent sites are presented in Fig. 2. The lithium atoms have coordination numbers (CN) of 15 (Li3) and 16 (Li1, Li2, Li4). Due to the site splitting in the centrosymmetric space group the coordination polyhedra of Li1 and Li4 are very similar (see also Table 3). Within these polyhedra, the Li–Li distances cover a relatively broad range from 268 to 307 pm. The shorter Li–Li distances are all somewhat smaller than in *bcc* lithium (304 pm) [60], similar to the situation in $LiRh_2Si_2$ (275 pm) [39]. In view of the highly ionic character (and thus small size) of lithium in $Li_{13.7}Rh_8Si_{18.3}$ (*vide infra*), these interactions may not be considered as bonding.

The shortest interatomic distances in the $Li_{13.7}Rh_8Si_{18.3}$ structure occur between the rhodium and silicon atoms. The atoms Rh, Si1 and Si2 presented in Fig. 2 have CN 12 in the form of strongly distorted icosahedra. This is also expressed by the low

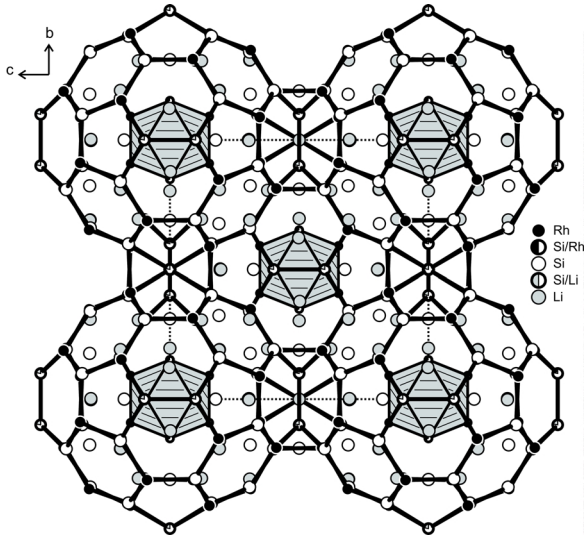

Fig. 4. Projection of the $Li_{13.7}Rh_8Si_{18.3}$ structure onto the *yz* plane. Relevant Rh–Si bonds are drawn, emphasizing the condensed M_{60} clusters. For details see text.

site symmetry 1. The Rh–Si distances range from 239 to 252 pm, close to the sum of the covalent radii of 242 pm [61]. A similar range (244 – 248 pm) has been observed for $LiRh_2Si_2$ [39]. We can therefore assume substantial covalent Rh–Si bonding in $Li_{13.7}Rh_8Si_{18.3}$. Besides we observe shorter Si1–Si2 distances of 242 and 249 pm. Although both distances are slightly longer than in elemental silicon (235 pm) [60], besides stronger Rh–Si we also observe weaker Si–Si bonding.

Together, the rhodium and silicon atoms build up a complex three-dimensional network. As emphasized in Fig. 3, the structure of $Li_{13.7}Rh_8Si_{18.3}$ contains a buckyball-type M_{60} cluster which encapsulates a slightly distorted icosahedron of *M*2 atoms. The lithium atoms as the most electropositive part of $Li_{13.7}Rh_8Si_{18.3}$ will largely have transferred their valence electrons to the rhodium and tin atoms, thus enabling formation of a polyanionic network. To a first approximation we can formulate $[Li_{13.7}]^{\delta+}[Rh_8Si_{18.3}]^{\delta-}$. The condensed network of the M_{60} clusters is shown in Fig. 4.

Acknowledgement

This work was financially supported by the Deutsche Forschungsgemeinschaft through SFB 458.

[1] H.-U. Schuster, *Naturwissenschaften* **1966**, *53*, 360.
[2] H. Pauly, A. Weiss, H. Witte, *Z. Metallkd.* **1968**, *59*, 47.
[3] H.-U. Schuster, D. Thiedemann, H. Schönemann, *Z. Anorg. Allg. Chem.* **1969**, *370*, 160.
[4] C.-J. Kistrup, H.-U. Schuster, *Z. Naturforsch.* **1972**, *27b*, 324.
[5] C.-J. Kistrup, H.-U. Schuster, *Z. Anorg. Allg. Chem.* **1974**, *410*, 113.
[6] W. Pobitschka, H.-U. Schuster, *Z. Naturforsch.* **1978**, *33b*, 115.
[7] U. Eberz, W. Seelentag, H.-U. Schuster, *Z. Naturforsch.* **1980**, *35b*, 1341.
[8] J. Drews, U. Eberz, H.-U. Schuster, *J. Less-Common Met.* **1986**, *116*, 271.
[9] R. Nesper, *Prog. Solid State Chem.* **1990**, *20*, 1.
[10] R. A. Huggins, in *Handbook of Battery Materials* (Ed.: J. O. Besenhard), Wiley-VCH, Weinheim, **1999**.
[11] R. Pöttgen, Zh. Wu, R.-D. Hoffmann, G. Kotzyba, H. Trill, J. Senker, D. Johrendt, B. D. Mosel, H. Eckert, *Heteroatom Chem.* **2002**, *13*, 506.
[12] R.-D. Hoffmann, D. Johrendt, Zh. Wu, R. Pöttgen, *J. Mater. Chem.* **2002**, *12*, 676.
[13] Zh. Wu, R.-D. Hoffmann, R. Pöttgen, *Z. Anorg. Allg. Chem.* **2002**, *628*, 1484.
[14] R.-D. Hoffmann, Zh. Wu, R. Pöttgen, *Eur. J. Inorg. Chem.* **2003**, 3425.
[15] Zh. Wu, B. D. Mosel, H. Eckert, R.-D. Hoffmann, R. Pöttgen, *Chem. Eur. J.* **2004**, *10*, 1558.
[16] Zh. Wu, R.-D. Hoffmann, D. Johrendt, B. D. Mosel, H. Eckert, R. Pöttgen, *J. Mater. Chem.* **2003**, *13*, 2561.
[17] Zh. Wu, H. Eckert, J. Senker, D. Johrendt, G. Kotzyba, B. D. Mosel, H. Trill, R.-D. Hoffmann, R. Pöttgen, *J. Phys. Chem. B* **2003**, *107*, 1943.
[18] Zh. Wu, H. Eckert, B. D. Mosel, R. Pöttgen, *Z. Naturforsch.* **2003**, *58b*, 501.
[19] P. Sreeraj, R.-D. Hoffmann, Zh. Wu, R. Pöttgen, U. Häussermann, *Chem. Mater.* **2005**, *17*, 911.
[20] P. Sreeraj, D. Johrendt, H. Müller, R.-D. Hoffmann, Zh. Wu, R. Pöttgen, *Z. Naturforsch.* **2005**, *60b*, 933.
[21] P. Sreeraj, D. Kurowski, R.-D. Hoffmann, Zh. Wu, R. Pöttgen, *J. Solid State Chem.* **2005**, *178*, 3420.
[22] P. Sreeraj, H.-D. Wiemhöfer, R.-D. Hoffmann, R. Skowronek, A. Kirfel, R. Pöttgen, *J. Solid State Chem.* **2006**, *179*, 355.
[23] P. Sreeraj, H.-D. Wiemhöfer, R.-D. Hoffmann, J. Walter, A. Kirfel, R. Pöttgen, *Solid State Sci.* **2006**, *8*, 843.
[24] P. Sreeraj, N. A. Kaskhedikar, H.-D. Wiemhöfer, J. Maier, R. Pöttgen, *Solid State Ionics* **2010**, *181*, 59.
[25] T. B. Massalski, H. Okamoto, P. R. Subramanian, L. Kacprzak (Eds.), *Binary Alloy Phase Diagrams*, 2nd ed. (version 1.0.), ASM International, NewYork, **1996**.
[26] W. Döring, W. Seelentag, W. Buchholz, H.-U. Schuster, *Z. Naturforsch.* **1979**, *34b*, 1715.
[27] O. I. Bodak, V. V. Pavlyuk, R. I. Andrusyak, B. Ya. Kotur, V. K. Pecharskii, V. A. Bruskov, *Kristallografiya* **1990**, *35*, 312; *Sov. Phys. Crystallogr. 35*, 173.

[28] V. V. Pavlyuk, O. I. Bodak, A. N. Sobolev, *Kristallografiya* **1991**, *36*, 883; *Sov. Phys. Crystallogr.* **1991**, *36*, 494.
[29] H.-U. Schuster, W. Seelentag, *Z. Naturforsch.* **1975**, *30b*, 804.
[30] V. V. Pavlyuk, D. G. Kevorkov, O. I. Bodak, V. K. Pecharskii, *Kristallografiya* **1995**, *40*, 178; *Crystallogr. Rep.* **1995**, *40*, 161.
[31] V. V. Pavlyuk, D. G. Kevorkov, O. I. Bodak, V. K. Pecharskii, *Kristallografiya* **1995**, *40*, 188; *Crystallogr. Rep.* **1995**, *40*, 171.
[32] V. V. Pavlyuk, D. G. Kevorkov, O. I. Bodak, V. K. Pecharskii, *Kristallografiya* **1995**, *40*, 185; *Crystallogr. Rep.* **1995**, *40*, 168.
[33] V. V. Pavlyuk, D. G. Kevorkov, O. I. Bodak, V. K. Pecharskii, *Kristallografiya* **1995**, *40*, 180; *Crystallogr. Rep.* **1995**, *40*, 163.
[34] H. Schönemann, H. Jacobs, H.-U. Schuster, *Z. Anorg. Allg. Chem.* **1971**, *382*, 40.
[35] H. Schönemann, H.-U. Schuster, *Rev. Chim. Minér.* **1976**, *13*, 32.
[36] M. S. Bailey, Q. Li, E. B. Lobkovsky, D. G. Hinks, J. F. Mitchell, *J. Solid State Chem.* **2008**, *181*, 30.
[37] V. V. Pavlyuk, D. G. Kevorkov, O. I. Bodak, V. K. Pecharskii, *Kristallografiya* **1995**, *40*, 183; *Crystallogr. Rep.* **1995**, *40*, 166.
[38] D. G. Kevorkov, V. V. Pavlyuk, O. I. Bodak, J. Stepien-Damm, *Kristallografiya* **1995**, *40*, 177; *Crystallogr. Rep.* **1995**, *40*, 160.
[39] T. Dinges, U. Ch. Rodewald, S. F. Matar, H. Eckert, R. Pöttgen, *Z. Anorg. Allg. Chem.* **2009**, *635*, 1894.
[40] T. Dinges, R.-D. Hoffmann, H. Eckert, R. Pöttgen, 12th European Conference on Solid State Chemistry, Abstract EM 030, Münster, **2009**, ISBN 978-3-936028-60-7.
[41] G. Bergman, J. T. L. Waugh, L. Pauling, *Nature* **1952**, *169*, 1057.
[42] G. Bergman, J. T. L. Waugh, L. Pauling, *Acta Crystallogr.* **1957**, *10*, 254.
[43] C. A. Guryan, P. W. Stephens, A. I. Goldman, F. W. Gayle, *Phys. Rev. B*, **1988**, *37*, 8495.
[44] M. Audier, J. Pannetier, M. Leblanc, C. Janot, J.-M. Lang, B. Dubost, *Physica B* **1988**, *153*, 136.
[45] M. Tillard-Charbonnel, C. Belin, *J. Solid State Chem.* **1991**, *90*, 270.
[46] M. Elding-Potén, S. Lidin, *J. Solid State Chem.* **1995**, *115*, 270.
[47] E. Todorov, S. C. Sevov, *Inorg. Chem.* **1997**, *36*, 4298.
[48] C.-S. Lee, G. J. Miller, *J. Am. Chem. Soc.* **2000**, *122*, 4937.
[49] C.-S. Lee, G. J. Miller, *Inorg. Chem.* **2001**, *40*, 338.
[50] B. Li, J. D. Corbett, *Inorg. Chem.* **2004**, 43, 3582.
[51] R. Pöttgen, Th. Gulden, A. Simon, *GIT Labor-Fachzeitschrift* **1999**, *43*, 133.
[52] K. Yvon, W. Jeitschko, E. Parthé, *J. Appl. Crystallogr.* **1977**, *10*, 73.
[53] G. M. Sheldrick, SHELXS-97, Program for the Solution of Crystal Structures, University of Göttingen, Göttingen (Germany) **1997**. See also: G. M. Sheldrick, *Acta Crystallogr.* **1990**, *A46*, 467.
[54] G. M. Sheldrick, SHELXL-97, Program for the Refinement of Crystal Structures, University of Göttingen, Göttingen (Germany) **1997**. See also: G. M. Sheldrick, *Acta Crystallogr.* **2008**, *A64*, 112.
[55] H. D. Flack, G. Bernadinelli, *Acta Crystallogr.* **1999**, *A55*, 908.
[56] H. D. Flack, G. Bernadinelli, *J. Appl. Crystallogr.* **2000**, *33*, 1143.
[57] H. Bärnighausen, *Commun. Math. Chem.* **1980**, *9*, 139.
[58] H. Bärnighausen, U. Müller, *Symmetriebeziehungen zwischen den Raumgruppen als Hilfsmittel zur straffen Darstellung von Strukturzusammenhängen in der Kristallchemie*, University of Karlsruhe and University/GH Kassel, Karlsruhe and Kassel, **1996**.
[59] U. Müller, *Z. Anorg. Allg. Chem.* **2004**, *630*, 1519.
[60] J. Donohue, *The Structures of the Elements,* Wiley, New York **1974**.
[61] J. Emsley, *The Elements*, Oxford University Press, Oxford **1999**.